Experimental Measurement of the Complex Young's Modulus on a CFRP Laminate considering the Constant Hysteretic Damping Model

D. Montalvão[a,1], R. A. L. D. Cláudio[b], A.M.R. Ribeiro[c], J. Duarte-Silva[b]

[a] School of Engineering and Technology, University of Hertfordshire, College Lane, Hatfield, AL10 9AB, UK

[c] Department of Mechanical Engineering, Escola Superior de Tecnologia de Setúbal, Polytechnic Institute of Setúbal, Campus do IPS, Estefanilha, 2910-761 Setúbal, Portugal

[b] Department of Mechanical Engineering, Instituto Superior Técnico, Technical University of Lisbon, Av. Rovisco Pais, 1049-001 Lisbon, Portugal

Abstract

When considering structural loss in vibration problems, the Young's modulus is a complex value that may be defined in the Argand plane as the vectorial sum of the real part of the Young's modulus itself and the loss modulus. By performing simple quasi-static force-displacement tests in a universal testing machine it is possible to experimentally measure the complex elastic modulus of a material, even if the loss factor is very small. In this work, the authors present the experimental results of the complex Young's modulus measurements on a specimen of a quasi-isotropic carbon fibre reinforced laminate, considering the constant hysteretic damping model. The setup is fully described and results are presented in detail, giving a special attention to the experimental problems so that this work can become a useful contribution for further studies.

Keywords: complex elastic modulus; complex Young's modulus; hysteretic damping; loss factor.

1. Introduction

[1] Corresponding author. Tel.: +44 (0) 1707 285387; fax: +44 (0) 1707 285086.

E-mail addresses: d.montalvao@herts.ac.uk (D. Montalvão), ricardo.claudio@estsetubal.ips.pt (R. A. L. D. Cláudio), aribeiro@dem.ist.utl.pt (A.M.R. Ribeiro), duarte.silva@estsetubal.ips.pt (J. Duarte-Silva),.

Assessment of the elastic and damping properties – complex modulus - of composite materials is of growing interest with the intensive current use of these materials in many modern engineering applications, from aerospace to sports components [1, 2].

When a material is deformed, elastic and internal frictional stresses appear. Generally, frictional stress is described as being analogous to the stress that results from the flow of a viscous fluid, that is, the friction stresses are considered proportional to the strain rate. But instead, experience shows that, for many structural materials, the friction stresses show a linear relation with the strain itself, at least for a wide range of frequencies [3]. The constant hysteretic damping model is the simplest way to describe this behaviour, assuming a complex Young's modulus.

A considerable amount of research has been done on the damping analysis in fibre-reinforced composite materials [4]. The damping loss factor can be estimated at the laminate level from the constituent materials and interfacial viscoelastic properties [5, 6, 7]. However, in the viscous model, it is frequency dependent, which differs from what is observed in most real structures which behaviour is closer to a frequency independent (or weakly dependent) dissipation mechanism [8]. The constant hysteretic damping model is often used to describe the dynamic behaviour of structures undergoing various loading conditions. This designation (hysteretic) results from the fact that such a mechanism closely describes the load deflection hysteresis behaviour of most materials.

Most often, the complex Young's modulus is defined as the vectorial sum of the Young's modulus (real part) and the loss modulus (imaginary part). This corresponds to a Cartesian representation of a vector in the Argand plane. This vector can also be represented by polar coordinates, with amplitude and phase, suggesting a lag, i.e., the tendency to react slowly to an outside force, or to not return completely to its original state.

The need to estimate the complex Young's modulus of a material is therefore important on several subjects of structural dynamics, such as modelling, updating, structural modification or damage detection. Concerning the field of damage detection, for instance, the main idea behind techniques that make use of vibration testing is the fact that the modal parameters (natural frequencies, mode shapes and modal damping) are functions of the physical parameters (mass, stiffness and damping) and it is thus reasonable to assume that the existence of damage leads to changes in the modal properties of the structure. Most often, the existing techniques assume that stiffness is a much more sensitive parameter to damage than damping. However, for structures made of composite materials, such as Carbon Fibre

Reinforce Polymers (CFRPs), there seems to be a tendency for the use of damping as the damage feature, since damping variations – associated to the dissipated energy – seem to be more sensitive to damage than the stiffness variations, mainly in what delamination is concerned [9]. For instance, Yam et al. [10] proposed to develop a method for the location and prediction of damage in carbon fibre reinforced plates by a combination of the measured modal damping and the computed strain energy distribution. More recently, Montalvão et al. [11] presented a method for locating damage in composite materials based on the comparison of both the modal damping factors and natural frequencies between a reference state and a damaged state. The damage location is assessed by a combination of two indexes that provide a geometrical distribution of the likelihood of the damage location. Furthermore, there are hints that different types of damage have diverse contributions to the modal parameters. For instance, a fibre breakage is more likely to affect stiffness whereas a debonding is more likely to affect damping. In other words, different types of damage affect the real and imaginary parts of the complex Young's modulus differently.

The purpose of this paper is to assess the complex Young's modulus of a material - in this case a CFRP laminate - using conventional experimental techniques and considering the constant hysteretic damping model. It is measured under conditions of cyclic or near-cyclic motion (force-displacement test). Because the imaginary part of the Young's modulus (damping factor) usually is very difficult to determine accurately, its value is estimated through classical logarithmic decrement techniques for comparison. It will be shown that the latter method has several problems that are not usually stressed out, and that the former can probably grant a better and more consistent estimate of the hysteretic damping of a material. Furthermore, it may be interesting to explore the hypothesis from Ribeiro *et al.* [12] that suggests the possibility of using the hysteretic model for the free vibration.

2. The complex Young's modulus

The concept of a complex Young's modulus (stiffness) in vibration problems with viscous or structural (hysteretic) damping is something that is known for decades. Most often the complex Young's modulus is defined as the vectorial sum of the Young's modulus (E', real part) and the loss modulus (E'', imaginary part):

$$E^* = E' + iE'' \tag{1}$$

To find the real and imaginary parts of the complex Young's modulus, it is easier if we first establish an analogy with the stiffness in a single degree of freedom system. Starting with the more conventional viscous damping model, the well-known second order differential equation of motion - for a single degree of freedom system - is given by:

$$m\ddot{x} + c\dot{x} + kx = Fe^{i\omega t} \tag{2}$$

where m is the mass, c is the damping coefficient, k is the stiffness, F is the amplitude of the oscillatory force and t is the time variable. When excited by a harmonic force at frequency ω, it can easily be proven (and most fundamental texts on vibration theory show it) that for each vibration cycle the system dissipates – through its viscous damper – a quantity of energy directly proportional to the damping coefficient, the excitation frequency and the square of the response amplitude X :

$$W_{diss} = \int_0^T f\dot{x}dt = \pi c\omega X^2 \tag{3}$$

where $T = 2\pi/\omega$ is the time period of oscillation. However, experimental evidence from tests performed on a large variety of materials show that damping due to internal friction (material hysteresis) is nearly independent of the forcing frequency but still proportional to the square of the response amplitude [13], i. e.:

$$W_{diss} \propto CX^2 \tag{4}$$

where C is a constant. Therefore, from equations (3) and (4) the equivalent damping coefficient is:

$$c_{eq} = \frac{C}{\pi\omega} = \frac{h}{\omega} \tag{5}$$

in which h is the hysteretic damping coefficient. In such conditions, equation (2) can be re-written as:

$$m\ddot{x} + \frac{h}{\omega}\dot{x} + kx = Fe^{i\omega t} \tag{6}$$

and because $\dot{x} = i\omega x$ for an harmonic vibration, this equation may be re-written as:

$$m\ddot{x} + k(1 + i\eta)x = Fe^{i\omega t} \tag{7}$$

where

$$\eta = h / k \tag{8}$$

is the hysteretic damping ratio. The quantity (in equation (7)):

$$k^* = k(1 + i\eta) \tag{9}$$

is the complex stiffness. Its real part, $k' = k$, represents the stiffness itself, and its imaginary part, $k'' = ik\eta = ih$, the loss factor.

The latter formulation (7) leads to the conclusion that the dissipated energy per cycle is independent of the forcing frequency. There are many other formulations that can be found in the literature. It must be stressed out that the one presented here is valid for forced vibrations (steady motion) with harmonic excitations.

With regard to the Young's modulus, it is the slope of a stress to strain relation, analogously to the stiffness that is the slope of a force to displacement relation. Thus, because the hysteretic damping ratio is dimensionless, the same formulation may be used for the complex Young's modulus, and equation (1) is therefore re-written as:

$$E^* = E(1 + i\eta) \tag{10}$$

which was the objective in the first place.

3. Determination of the complex Young's modulus by means of cyclic loading

3.1. Real part

A tensile test, also known as *tension test* or *force-displacement test*, is a fundamental type of mechanical test that can be performed on a material. Tensile tests are simple, relatively inexpensive, fully standardized, and allow determining the engineering constants of a material. Engineering constants (sometimes known as *technical constants*) are generalized Young's

moduli, Poisson's ratios, shear moduli and some other behavioural constants. These constants are measured in simple tests such as uniaxial tension or pure shear tests [14]. Most simple material characterization tests are performed with a known load or stress. The resulting displacement or strain is then measured. The engineering constants are generally the slope of a stress-strain curve (elastic or Young's modulus) or the slope of a strain-strain curve (Poisson's ratio) for $\sigma_1 \neq 0$ and all other stresses are zero. Keeping in mind Hooke's law, the Young's modulus E_1 in the longitudinal direction of a specimen is usually determined by:

$$E_1 = \frac{\sigma_1}{\varepsilon_1} \tag{11}$$

where σ_1 and ε_1 are the stress and strain, respectively, in the longitudinal direction.

It must be stressed out that this is the simplest way of presenting the Young's modulus (or the stiffness of a material), as it ignores the hysteresis of the material, i.e., the fact that the maximum stress does not occur for the maximum strain. This important aspect of the formulation will be briefly discussed in section 3.3.

3.2. Imaginary part

The experimental measurement of the hysteretic damping factor can be carried out by means of cyclic force-displacement tests in the elastic domain [12]. Following the reasoning presented before and from equations (5) and (8), equation (3) can be re-written as:

$$W_{diss} = \int_0^T f\dot{x}dt = \pi k \eta X^2 \tag{12}$$

The integral of the force along the displacement (recall that $\dot{x}dt = dx$), corresponds to the non-conservative work done per cycle. This shows up as something similar to an elongated ellipsis in a force vs displacement plot. In other words, damping can be seen as a mechanism that introduces a lag between the input (force) and response (displacement) during a traction-compression cycle. Although Rowett's experiments [15] showed a non-elliptical hysteresis curve with sharp endpoints in steel, for low-damping structures at low stress, the approximation that the hysteresis curve is elliptical seems to be good [13]. Thus, by taking this approximation into consideration and from equation (12), the hysteretic damping factor can be evaluated from a force-displacement test by using the following relationship:

$$\eta = \frac{ellipse\_area}{\pi k X^2} \tag{13}$$

Another way of writing an equation for the hysteretic damping factor starts from the representation of the complex stiffness k^* (equation (9)) in a vector diagram, with the real part $k' = k$, and the imaginary part, $k'' = ik\eta$. In this case, the following relationships may be derived for the phase angle θ between k^* and the x:

$$\tan\theta = \frac{k'}{k''} = \frac{\eta k}{k} = \eta \tag{14}$$

For the most common materials used in engineering applications, the damping factor is usually small ($\eta < 0.1$) and equation (14) may be re-written in such a way it expresses the so-called *hysteresivity* (meaning lag):

$$\eta = \tan\theta \cong \theta, (\eta < 0.1) \tag{15}$$

For a matter of simplicity during this text, equation (13) will be referred to as the *areas method* and equation (14) as the *phase method*, but bear in mind that they both constitute approximated estimates of the hysteretic damping factor under uniaxial loading.

3.3. Some considerations on the validity of the approximations taken

All the previous formulation considers a sharp ellipse on its tip-ends, which is not true. In fact, the point of maximum/minimum displacement X does not correspond to the point of maximum/minimum force F in the hysteresis cycle, as shown in figure *1*. In other words, in the previous equations, the "stiffness" k is not the relationship between the maximum force and the maximum displacement, as it is assumed in Hooke's law. Lazan [13] calls k' the storage modulus, the slope of the line between point O and the point of the maximum displacement amplitude; and calls $|k^*|$ (the slope of) the maximum point modulus, which is the slope of the line between point O and the point where the extensions of the maximum force and maximum displacement amplitudes would cross.

However, because the damping ratio is very small in most applications, for practical purposes, the approximations that $\left|k^*\right| \cong k' \cong k$ and that $\left|E^*\right| \cong E' \cong E$ can generally be used without loss of accuracy.

FIGURE 1 IS SUGGESTED HERE

4. Test setup and procedural guidelines

The quasi-isotropic specimen is made from a $[0/45/135/90]_S$ layup. The designation *quasi-isotropic* is in accordance to ASN A 4135:1997 standard and to [16]. As such, the material may be treated as having the same properties at every direction. Each layer is a woven prepreg constituted by Hexcel® G803 3K 5H satin carbon fibre impregnated in HexPly® 200 phenolique matrix (200/40%/G803).

The specimen used for the hysteretic damping assessment has a rectangular cross section of 25x2mm and a length of 50mm between grips (figure *2*). The length of the specimen was chosen to be as short as possible (but sufficiently large to accommodate the strain gauges and with enough room for the machines' clamps), to avoid buckling when compressive forces are applied during the force-displacement tests.

FIGURE 2 IS SUGGESTED HERE

FIGURE 3 IS SUGGESTED HERE

Experimental quasi-static force-displacement tests are performed in a universal servo-hydraulic testing machine, INSTRON® 1342 under load control. Figure *3* schematically represents the measurement chains of force and strain. Different force amplitudes and frequencies were used; 30 sinusoidal cycles being performed and recorded for each condition. The acquired data were force and strain at a sampling rate of 1000 points per cycle.

The force was measured with a 250kN load cell calibrated in the 1 kN to 100 kN load range according to ISO 7500-1:2004 class 0.5. To measure the strain accurately, the specimens are instrumented with two strain gauges (HBM® LY11-350Ω) bonded at opposing faces of the specimen in order to account for some bending that may occur during testing. The value of the

strain[2] under axial loading is the averaged value of these two strains. Nevertheless, the machine was verified for misalignment beforehand (including concentricity) according to the manufacturer's recommendations. A calibration plate specimen with two strain gauges attached (one bounded at each face) was used to check if the grips introduced bending when the specimen was clamped.

In order to ensure that the load was properly applied to the specimen, the Proportional-Integral-Derivative (PID) values for feedback control of the testing machine were adjusted for each loading frequency (0.1, 1 and 10 Hz).

The signals were not filtered, in order to avoid any phase disturbance between them. The time domain hardware filters would introduce phase shifts, which is not desirable when the phase between two signals is wanted to be accurately assessed. Digital RFI filters introduce a constant phase shift and can be used; however, although the data naturally exhibited some level of noise, the integration process over 30 cycles averaged it out and the authors took the decision not to use any filters. For the experimental data so obtained, a force-strain plot was used to compute numerically the area of the ellipse for each cycle (figure *4*, for a test performed at 0.1Hz, although the 30 superimposed "ellipses" are too narrow to be visible) and the phase angle between the two signals was determined from a force and strain vs. time plot.

FIGURE 4 IS SUGGESTED HERE

As mentioned before, tests were performed at different frequencies; however, for a 10Hz testing frequency the ellipse shown in figure *4* turned out to be much wider, as can be observed on the left side of figure *5*. Although the immediate conclusion is that damping is having a considerable variation with frequency (contrary to the constant hysteretic model assumption), it was observed that the damping "presented a negative value", meaning that the force was suffering from a delay relatively to the displacement. That can be seen on the right side of the same figure where both functions, force and strain, are plotted in the time domain. Measurement chain bias was considered a possible cause for this abnormality. A force delay of

---

[2] Because the hysteretic damping factor η is dimensionless and recalling that the $ellipse\_area$ and stiffness k depend on the displacement X, the longitudinal strain can be used instead in the force-displacement tests when one wants to obtain the damping factor only. This can be shown by resorting to dimensional analysis over equation (13).

approximately 0.1ms was measured in the test machine by impacting the two grips, one against the other without any specimen. This delay results from the different signal conditioners that are used for the force and strain measurements.

FIGURE 5 IS SUGGESTED HERE

In fact, different electronic equipment, with different processing times, are used to process the force and strain signals, introducing a phase shift; although small, it may be significant enough to pollute the results when it is added to the one (also small) originated by the damping in the cyclic force-displacement process.

Tests were also carried out with different loading cases: traction-compression (±2kN, ±3kN and ±4kN), compression (-0.5kN to -3.5kN) and traction (+0.5kN to +6.5kN).

5. Results

5.1. Determination of the real part of the complex Young's modulus under cyclic loading

The determination of the real part of the Young's modulus offers no difficulties, as for linear materials and considering the approximations assumed for small damping ratios it is the slope of a stress vs strain chart. Some examples are presented in figure 6, where it can be seen that the electronic lag is only making the ellipse wider, with negligible effects on the slope. A summary of the whole results produced is shown in table 1.

FIGURE 6 IS SUGGESTED HERE

TABLE 1 IS SUGGESTED HERE

Observation of figure 6 and table 1, leads to the following comments:

- The correlation coefficients (R^2) are barely one. This corroborates the hypothesis that the data may indeed be treated as linear, for the sake of the real part of the Young's modulus, even if at 10 Hz the ellipse is quite visible;
- There seems to be a systematic tendency for the Young's modulus to present larger values as the frequency increases, although the differences are very small (less than

0.5%). Several explanations might be behind this, for instance the fact that the test is not truly static, but it is believed that the machine's PID for feedback control also has a strong influence, especially at larger frequencies;

- It cannot be ignored that the Young's modulus estimates seem to suffer very slight variations with the mean load and cycles type (traction or compression), but there is not sufficient data for more consistent conclusions.

The quality of these results may be assessed by comparing with other results. For instance, a theoretical value of 48.4 GPa for the undamped Young's modulus of the CFRP under study, using Classical Laminate Theory (CLT) and the rule of mixtures was previously determined [17]. In that case, only the properties of a unidirectional layer were available and the approximation that each satin weave layer was composed by two plies of orthogonal unidirectional layers with half the thickness was made. Nevertheless, this value is very close to the one so obtained here (2% difference), which means a very good agreement between the theoretical and experimental results.

5.2. Determination of the imaginary part – loss factor - of the complex Young's modulus

As the signal conditioners induced phase shift that is independent of the frequency load, for the frequency ranges considered, it was decided to perform tests at 0.1, 1 and 10 Hz and to extrapolate the damping factor obtained to 0 Hz using a least-squares fit. Thus, some estimations of the hysteretic damping by means of both the areas and phase methods (equations (13) and (14)) are shown in figure *7*, where the intersection of the linear fit to the vertical axis corresponds to the hysteretic damping factor (represented by the independent term in the linear-fit equation). A summary of the results produced with both methods is shown in table 2.

FIGURE 7 IS SUGGESTED HERE

TABLE 2 IS SUGGESTED HERE

Observation of figure *7* and table 2 leads to the following comments:

- Despite the fact that a sample of only 3 measurements at different frequencies was used to evaluate the linear fit, the correlation coefficients (R^2) were very close to 1 in all cases;
- The angular coefficients of the linear fits are approximately the same (≈-0.007) for each setup. This suggests that the delay introduced by the electronics is constant and independent of the measurement setup used;
- The results showed differences not larger than 10% (relatively to the mean value), which means a reasonable agreement for both methods;
- The phase method seems to have a tendency to produce smaller values for the hysteretic damping factor than the areas method. However, the discrepancy of the hysteretic damping factor between the one obtained with the phase method (0.00267) and the one obtained with the areas method (0.00280) is smaller than 5%, which is believed to be an acceptable result, considering the magnitudes of the values.

These results sustain the assumption that the measurement chain could be the source for the inconsistency of the raw results.

5.3. Validation of the results concerning the hysteretic damping factor

As reported above, there were a few electronic and control problems during the measurement of the hysteretic damping factor under cyclic loading. Still, even though they have been tackled, this raises the question about whether the hysteretic damping values so obtained are reliable enough. So, it was decided to perform a set of tests, with different methods and using different materials, for comparison and validation purposes.

5.3.1. Determination of the imaginary part – loss factor - of the complex Young's modulus by means of free decay testing

By definition, the logarithmic decrement is the natural logarithm of the decay rate (ratio between two amplitudes x_i and x_{i+1} spaced by n cycles):

$$\delta = \frac{1}{n} \ln \frac{x_i}{x_{i+1}} \tag{16}$$

In most applications the damping ratio is very small and the logarithmic decrement can be approximately given by:

$$\delta = 2\pi\xi \tag{17}$$

where ξ is the viscous damping factor. Since the model considered so far has been the hysteretic model, it may be interesting to explore the hypothesis from Ribeiro *et al.* [12] that suggests the possibility of using the hysteretic model for the free vibration. If such suggestion is considered, the logarithmic decrement would be approximately given by:

$$\delta = \pi\eta \tag{18}$$

Within this hypothesis, free-vibration tests were performed to obtain the experimental free decay behaviour of a cantilevered beam. A reflective tape was attached on the free tip of the cantilevered beam (as previously shown in figure *2*) and the time response obtained in terms of the velocity (a Laser Doppler Vibrometer was used - Polytec® Controller OFV-2802i and Polytec® Interferometer OFV-508). In order to avoid as much as possible any changes introduced by the data processing, the velocity itself was used. The initial conditions were introduced so that a displacement on the free tip of the specimen was high enough to produce a measured signal of good quality (high signal-to-noise ratio) but still within the linear behaviour range, i.e., $\dot{x}(t=0) \approx 0mm/s$ and $x(t=0) \approx 1mm$. The beam was clamped to a much stiffer and heavier structure, using 45mm of its length. The logarithmic decrement was measured using 2 amplitudes spaced by 49 cycles, and repeated, for each block of 50 amplitudes, thus providing a total of 350 values for the hysteretic damping factor (amplitude 1 with amplitude 50, amplitude 2 with amplitude 51, amplitude 3 with amplitude 52, and so on). The first 250ms of the time-signal used to compute the hysteretic damping factor for the free vibration decay is plotted in figure *8*, showing that the influence of higher frequency modes already vanished. The results for the hysteretic damping factor obtained by the free-decay testing are shown in figure *9*.

FIGURE 8 IS SUGGESTED HERE

FIGURE 9 IS SUGGESTED HERE

It is clear that the damping factor is not constant with time, starting with a value of 0.0043 and having an asymptotic tendency to a value of 0.0027, very close to the one obtained with the force-displacement test.

Nevertheless, the same test was repeated, but this time the clamping force was increased (although it was not quantified), leading to the results shown in figure *10*.

FIGURE 10 IS SUGGESTED HERE

As expected, the clamping mechanism is performing an important role on the process of the free vibration of the cantilevered specimen (note that the specimen was not moved from its original position and only the clamping force was increased). This time, the changes on the hysteretic damping factor are not as large (0.0028 in the beginning to 0.0024 at the end of the time signal), but it still represents a considerable variation (17%).

The damping factor seems once more to converge when it achieves smaller amplitude levels of vibration and, in both cases, the hysteretic damping factor seems to oscillate, which may be a consequence of the influence of the clamping structure itself. However, it was not possible to assess how much energy went into the clamps.

Other phenomena interfering with the experiment (i.e., that were not considered in the model and that were not measured) may be aerodynamic damping and material non-linearity that are more evident for larger amplitudes of vibration [15].

5.3.2. Validation of the test methods (cyclic loading and free decay) for damping assessment

To gain better insight about the methods themselves, it was decided to repeat the whole process, this time using an 800mm length steel beam with a 25x6mm^2 rectangular cross section. The purpose was to confirm if the boundary conditions on the free-vibration tests were, in fact, responsible for the variation of the damping factor, or if it was the composite material itself the reason for such a behaviour. First, a force-displacement test, ranging from +1 to +10kN was performed (to avoid buckling, compressive loading was not used), at three different frequencies of 0.1Hz, 1Hz and 10Hz, producing an estimation of the hysteretic damping factor of 0.00243 with the areas method and 0.00218 with the phase method. After that, a free-vibration test was conducted, following the same procedure. A variable hysteretic damping ranging from 0.0036 to 0.0023 was obtained, with a slight convergence in the end of

the time signal. Since the convergence happens for smaller amplitudes of vibration (thus less air damping and lower stresses aggravating the non-linear effects), the value to be considered is that obtained for the smaller amplitudes; this value (0.0023) is within the range obtained for the force-displacement tests, thus supporting the assumed hypothesis.

To further increase the confidence in the results, it was decided to perform similar tests on a material with larger damping: a high density poly-urethane beam with a 25x15mm^2 rectangular cross section. Final results for the composite specimen, steel beam and poly-urethane beam are presented in table *3*.

TABLE 3 IS SUGGESTED HERE

These final results show that all the three methods provide coherent results, given some of the previous considerations, for all the materials put under test. As a result, a confident value for the CFRP damping factor was obtained.

6. Conclusions

Various results have been presented, concerning the complex Young's modulus measurement on a CFRP laminate. For the CFRP laminate under study, the (averaged) value obtained was:

$$E^* \cong 49.4(1+0.00262i) \cong 49.4+0.129i(GPa)$$

To accomplish this objective, a force-displacement (cyclic loading) test was used. It was shown that the experimental assessment of the imaginary part of the complex Young's modulus (loss factor) presents several difficulties that cannot be neglected, even when dealing with free-vibration testing on a cantilevered beam for validation. In summary, the following conclusions can be drawn:

- For the case of the force-displacement testing, an approach based on a linear fit along the frequency was used to minimize the problems introduced by the measurement chain, showing a good agreement between the results;
- The fact that the correlation coefficients are close to unity in the linear-fits, shows that, for the frequency range considered, the constant damping model seems suitable for the global damping mechanism in a CFRP;

- For different loading conditions, no considerable changes on the hysteretic damping factor were observed, which shows that - for the force-displacement setup conditions - the material performed linearly;
- On free-vibration testing, the boundary conditions play an important role on the results. In the case of a cantilevered beam, the clamping force has a strong influence on the measurements, as well as other phenomena like air damping;
- The best region of the time domain decay to estimate the hysteretic damping factor of a cantilevered beam is the one with the lowest displacement amplitudes, but high enough for an acceptable signal-to-noise ratio. There is a considerable variation on the hysteretic factor with time, although it seems to converge to similar values to those obtained in the cyclic force-displacement test;
- When compared to the free vibration test, the force-displacement test is less influenced by external factors if the measurement setup is carefully prepared and corrective approaches are followed;
- The force-displacement test seems to be more reliable to evaluate the damping factor of a material than the free-vibration testing, according to the previous conclusions. On the free vibration testing the structural damping measured is influenced by many other factors that are not taken into account in the model.

Acknowledgements

The authors gratefully acknowledge Prof. João Travassos and Eng. Paulo Caldeira from Instituto Superior de Engenharia de Lisboa of the Polytechnic Institute of Lisbon for the use of their autoclave and consumables for the production of CFRP specimens.

The authors would also like to acknowledge Fundação para a Ciência e a Tecnologia (FCT) and the European Social Fund under the III Community Support Framework, for financial support through grant reference number SFRH / BD / 27329 / 2006.

References

[1] Matter M, Gmür T, Cugnoni J, Schorderet A. Numerical-experimental identification of the elastic and damping properties in composite plates. Compos Struct 2009; 90:180-7.

[2] Liao Y, Wells V. Estimation of complex modulus using wave coefficients. J Sound Vib 2006; 295:165-93.

[3] Crandal S. The role of damping in vibration theory. J Sound Vib 1970; 11:3-18.

[4] Chandra R, Singh SP, Gupta. Damping studies in fiber-reinforced composites – a review. Compos Struct 1999; 46:41-51.

[5] Zhang SH, Chen HL. A study on the damping characteristics of laminated composites with integral viscoelastic layers. Compos Struct 2006; 74:63-9.

[6] Berthelot JM, Assarar M, Sefrani Y, Abderrahim EM. Damping analysis of composite materials and structures. Compos Struct 2008; 85:189-204.

[7] Sarlin E, Liu Y, Vippola M, Zogg M, Ermanni O, Vuorinen J, Lepistö T. Vibration damping properties of steel/rubber/composite hybrid structures. Compos Struct 2012; 94:3327-35.

[8] Silva JMM, Maia NMM. Theoretical and Experimental Modal Analysis. Research Studies Press, Somerset, 1997.

[9] Montalvão D, Maia NMM, Ribeiro AMR. A review of vibration-based structural health monitoring with special emphasis on composite caterials. Shock Vib Dig 2006; 38:295-324.

[10] Yam LH, Wei Z, Cheng L. Nondestructive detection of internal delamination by vibration-based method for composite plates. J Composite Mater 2004; 38:2183-98.

[11] Montalvão D, Ribeiro AMR, Duarte-Silva JAB. Experimental assessment of a modal-based multi-parameter method for locating damage in composite laminates. Exp Mech 2011; 51(9):513-20.

[12] Ribeiro AMR, Silva JMM, Maia NMM, Reis LFG, Freitas MJM. Free vibration response using the constant hysteretic damping model. In: Proceedings of the 11th International Conference on Vibration Engineering, Timisoara, Romania, 2005, p. 65-70.

[13] Lazan BJ. Damping of materials and members in structural mechanics. Pergamon Press, Oxford, 1968.

[14] Jones RM. Mechanics of composite materials. Taylor & Francis, Philadelphia, 1999.

[15] Rowett FE. Elastic hysteresis in steel. Proceedings of the Royal Society of London A 1914; 89(614):528-43.

[16] Reis LFG. Análise do dano devido a cargas de impacto em materiais compósitos. MSc thesis, Instituto Superior Técnico, Technical University of Lisbon, 1996 [in Portuguese].

[17] Montalvão D. A modal-based contribution to damage location in laminated composite plates. PhD thesis, Instituto Superior Técnico, Technical University of Lisbon, Portugal, 2010.

Figure captions

Fig. 1: Hysteresis cycle (partial view).

Fig. 2: Carbon fibre laminate specimen.

Fig. 3: Force-displacement quasi-static test: a) testing hardware; b) Specimen inside the testing machine.

Fig. 4: Force-strain plot for a load magnitude of ±3kN and a frequency of 0.1Hz.

Fig. 5: Force and strain for a load magnitude of ±3kN and a frequency of 10 Hz. Left: force-strain plot; Right: superimposed force-time and strain-time plots.

Fig. 6: Some examples of stress-strain charts for the determination of the real part of the complex Young's modulus.

Fig. 7: Numerical extrapolations for the estimation of the hysteretic damping factor: Upper row: areas method; Lower row: phase method.

Fig. 8: Experimental free decay velocity (cantilevered CFRP laminate).

Fig. 9: Hysteretic damping along superimposed time blocks of 50 cycles.

Fig. 10: Hysteretic damping along superimposed time blocks of 50 cycles (larger clamping force).

Table captions

Table 1: Young's moduli obtained in the force-displacement tests (GPa).

Table 2: Hysteretic damping factor values obtained in the force-displacement tests.

Table 3: Hysteretic damping results summary.

Table 1

Cycles type	Load (kN)	0.1 Hz	1 Hz	10 Hz
Traction-Compression	-2 to +2	49.22	49.37	49.41
Traction-Compression	-3 to +3	49.20	49.35	49.37
Traction-Compression	-4 to +4	49.14	49.31	49.33
Compression-Compression	-0.5 to -3.5	48.65	48.81	48.79
Traction-Traction	+0.5 to +6.5	50.03	50.19	50.27
	Average Young's	49.25	49.41	49.43
	Modulus (GPa)		49.4	

Table 2

Cycles type	Load (kN)	Areas method	Phase method
Traction-Compression (1)	-2 to +2	0.00300	0.00266
Traction-Compression (2)	-3 to +3	0.00255	0.00261
Traction-Compression (3)	-4 to +4	0.00267	0.00249
Compression-Compression	-0.5 to -3.5	0.00279	0.00264
Traction-Traction	+0.5 to +6.5	0.00300	0.00293
	Average Damping	0.00280	0.00267

Table 3

	Areas method	Phase method	Free-vibration	Average
CFRP	**0.0028**	**0.0027**	**0.0024**	**0.0026**
Steel	0.0024	0.0022	0.0023	0.0023
High density poly-urethane	0.017	0.018	0.019	0.018

Figure 1

Click here to download high resolution image

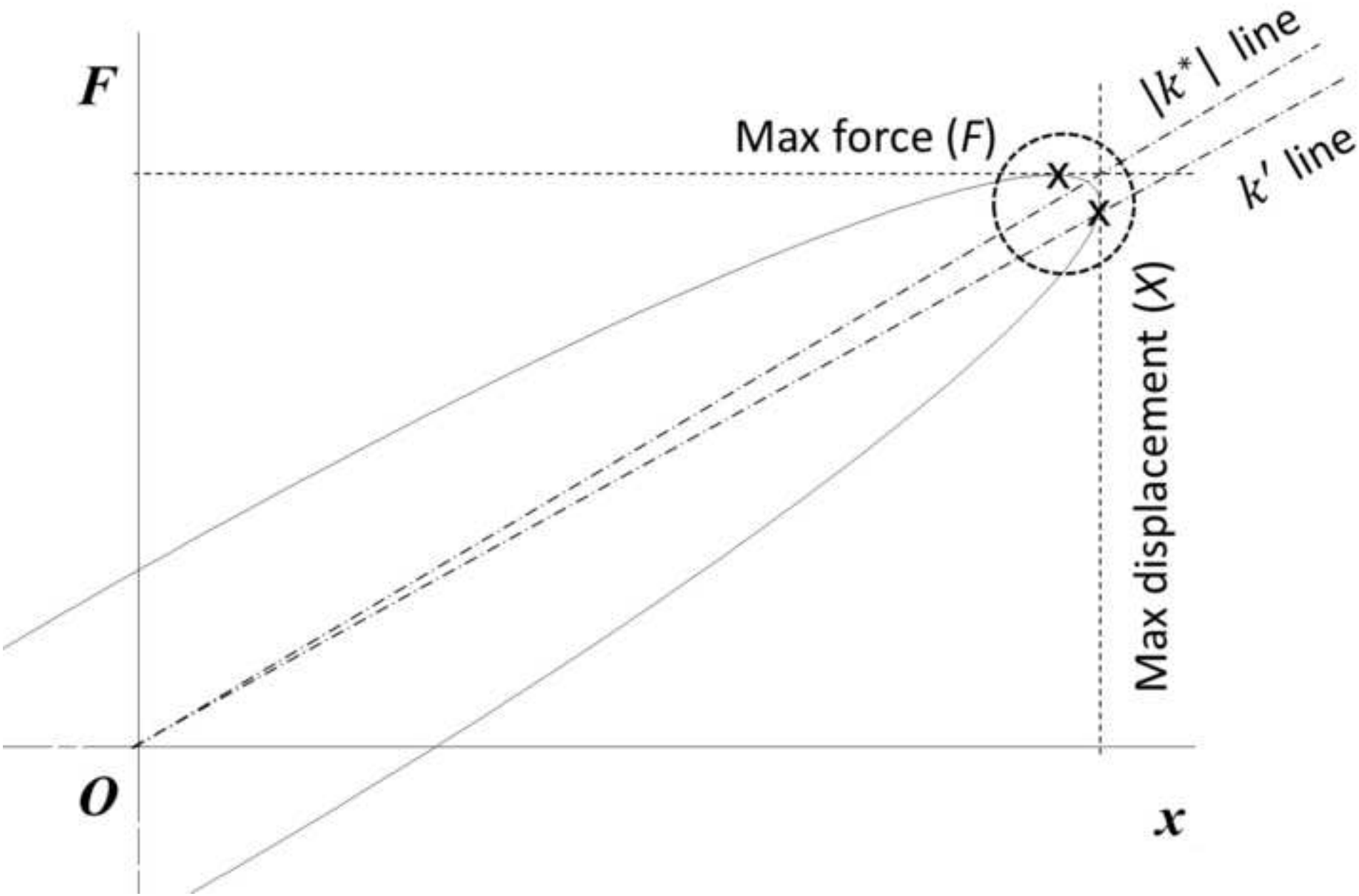

Figure 2 ONLINE

Click here to download high resolution image

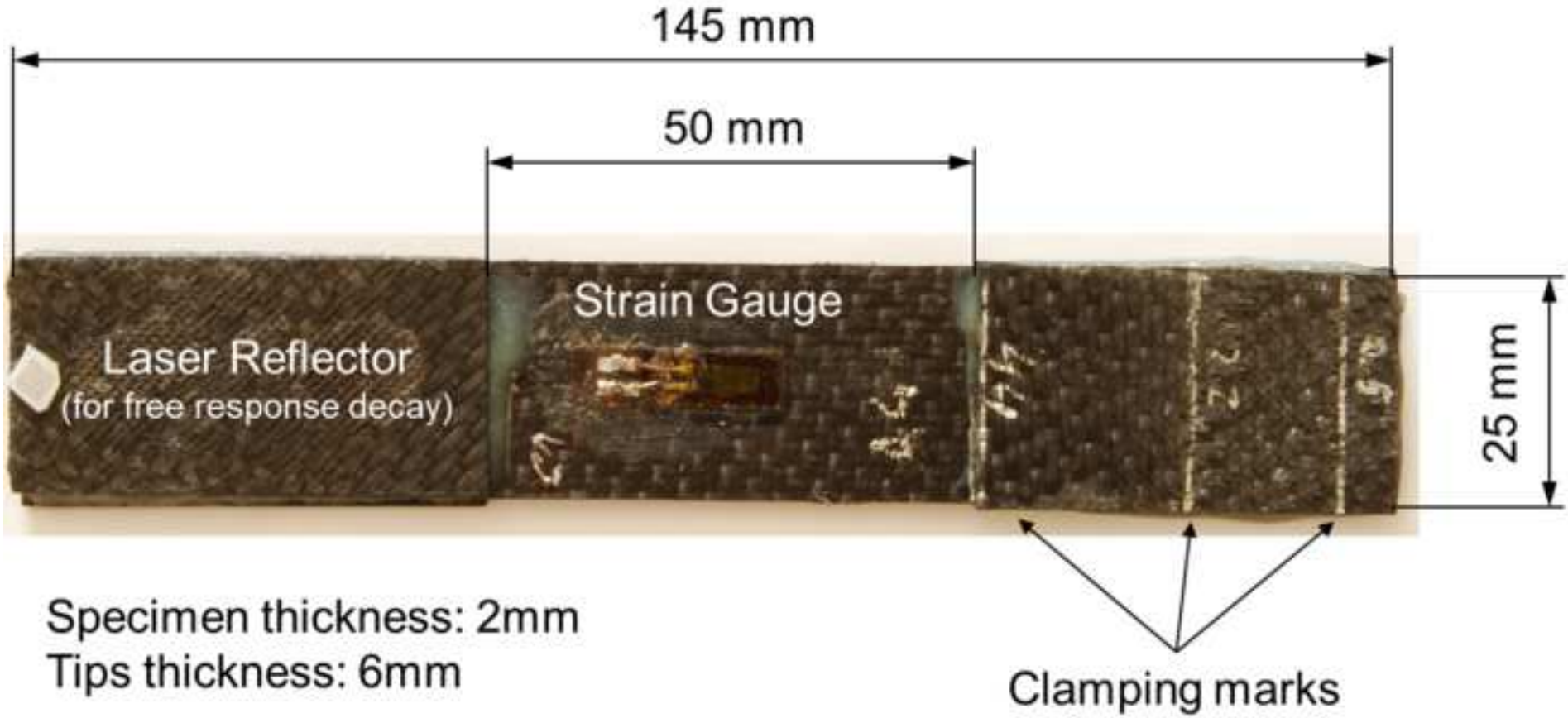

Figure 2 PAPER

Click here to download high resolution image

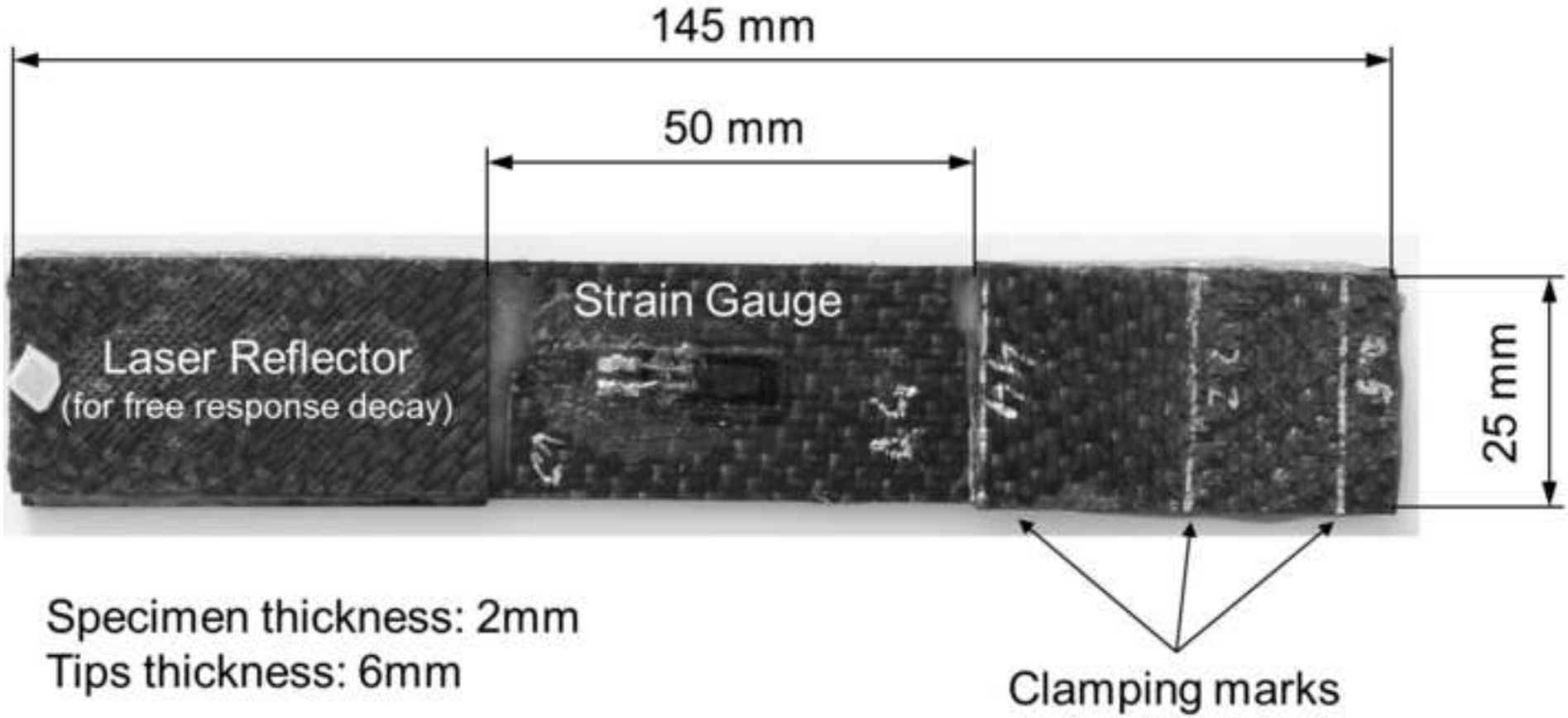

Figure 3 ONLINE

Click here to download high resolution image

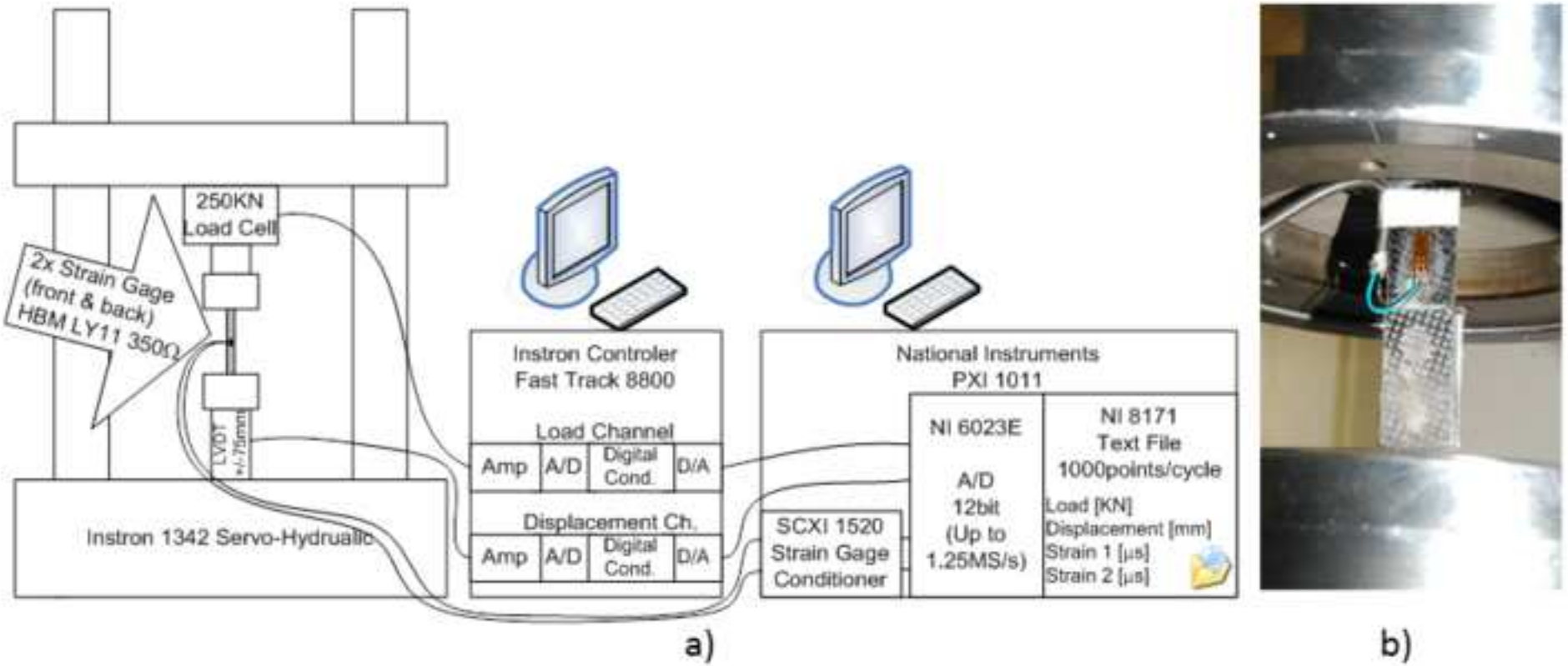

Figure 3 PAPER

Click here to download high resolution image

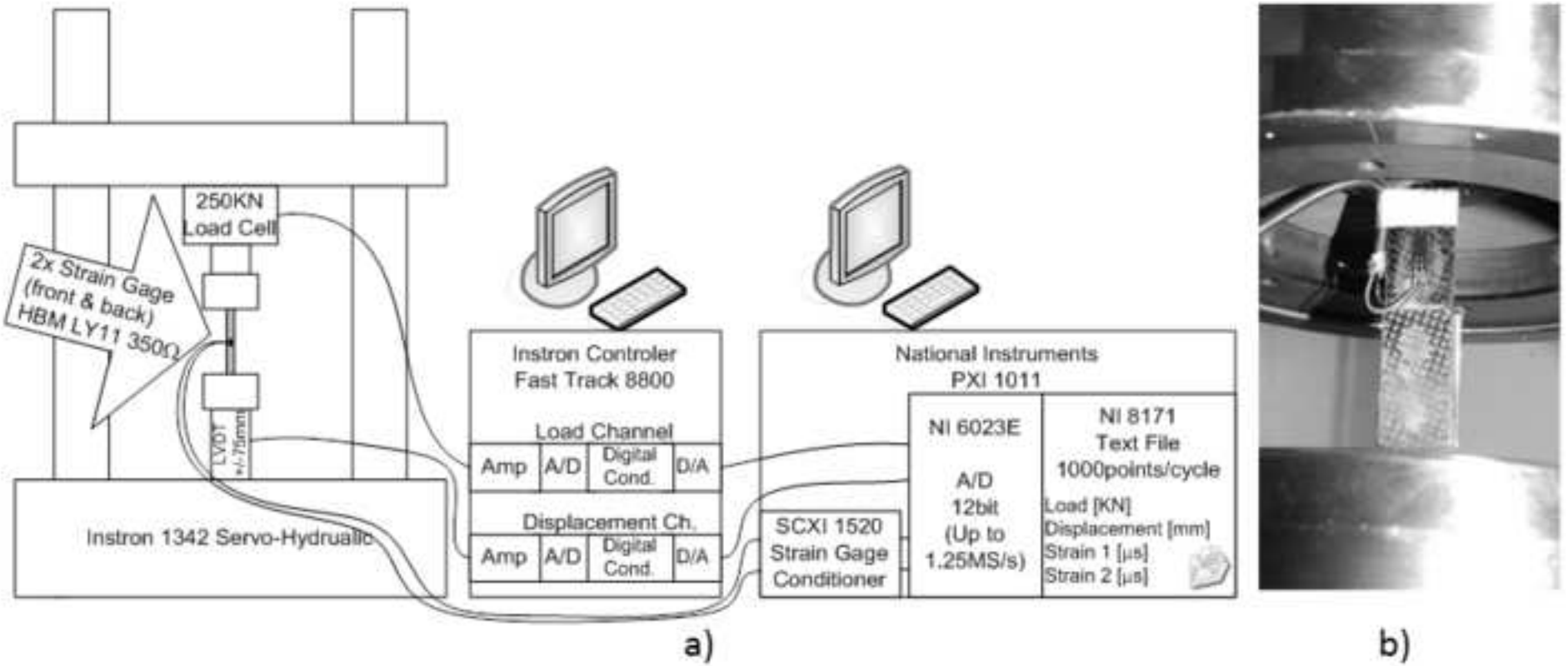

Figure 4 ALL_VERSIONS
Click here to download high resolution image

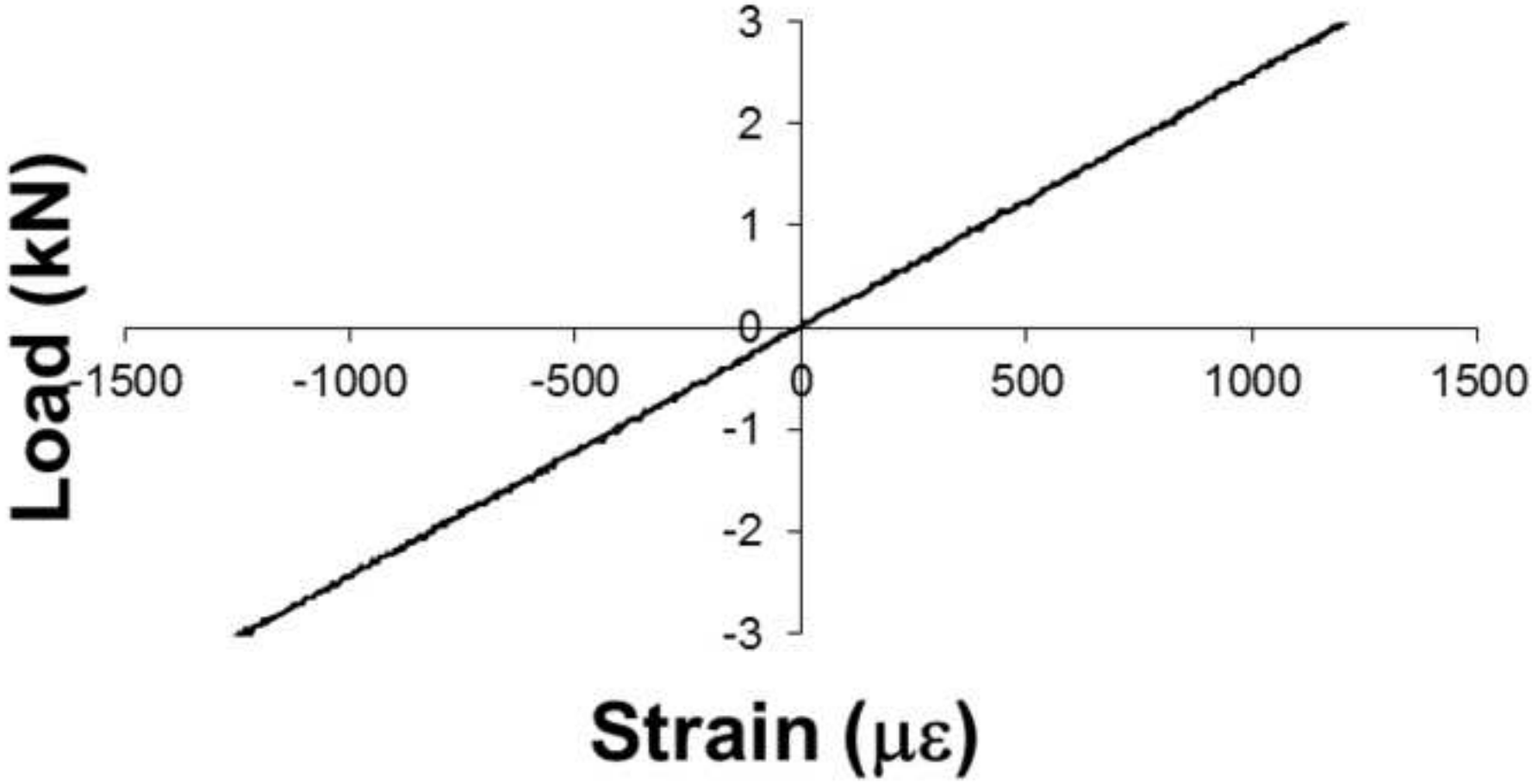

Figure 5 ALL_VERSIONS
Click here to download high resolution image

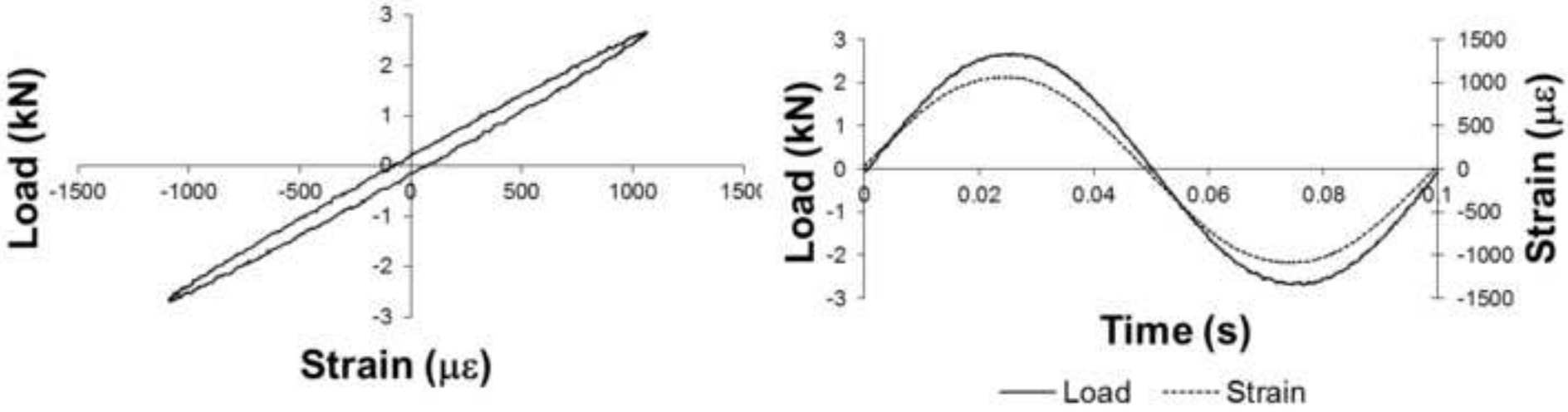

Figure 6 ALL_VERSIONS
Click here to download high resolution image

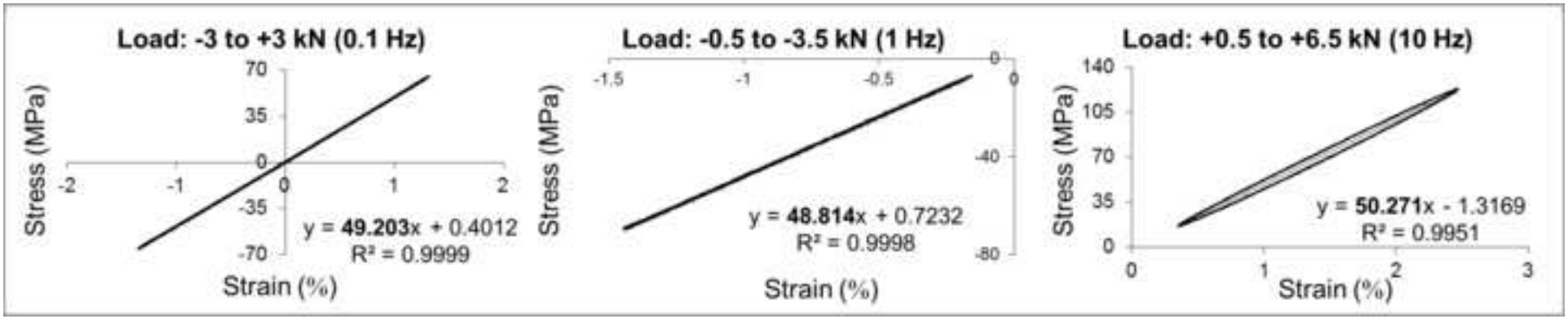

Figure 7 ALL_VERSIONS
Click here to download high resolution image

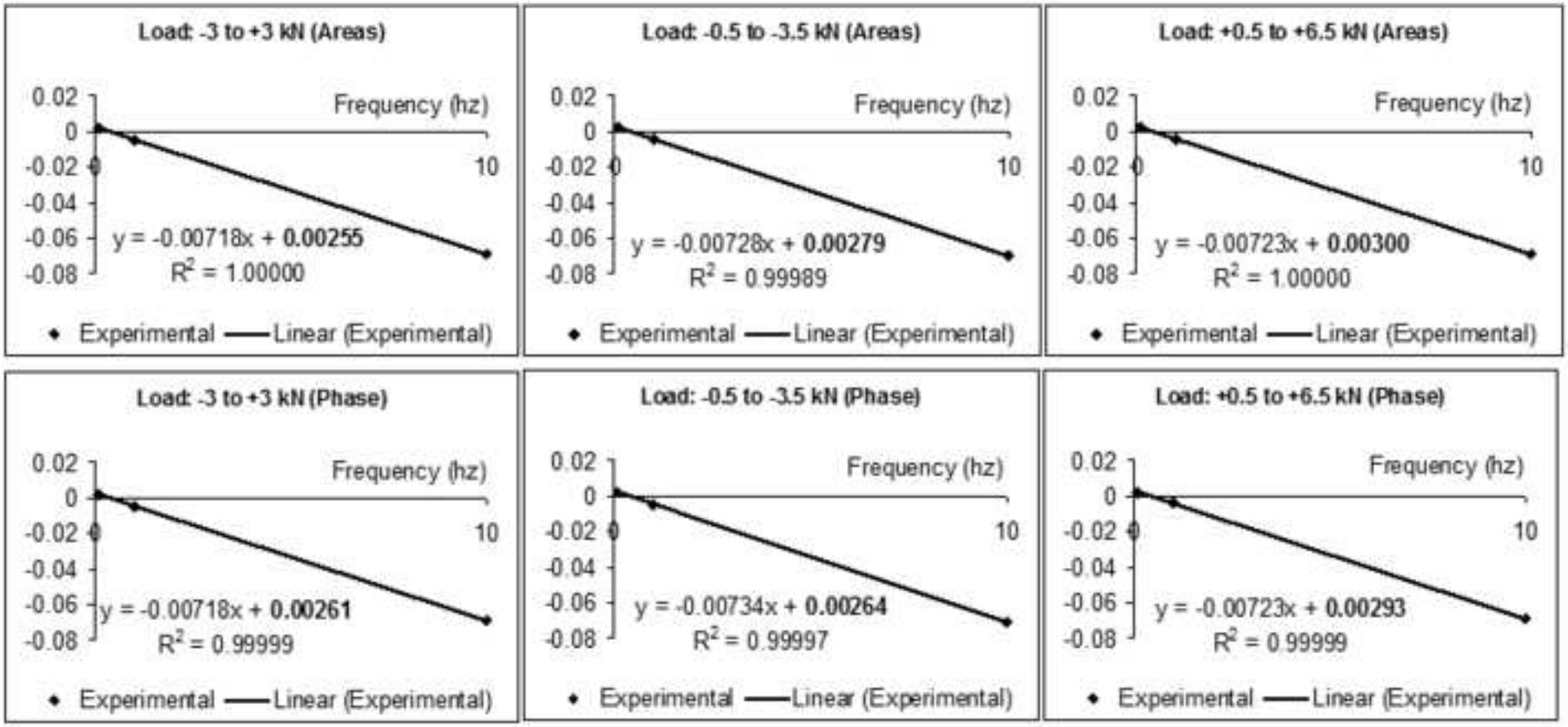

Figure 8 ALL_VERSIONS
Click here to download high resolution image

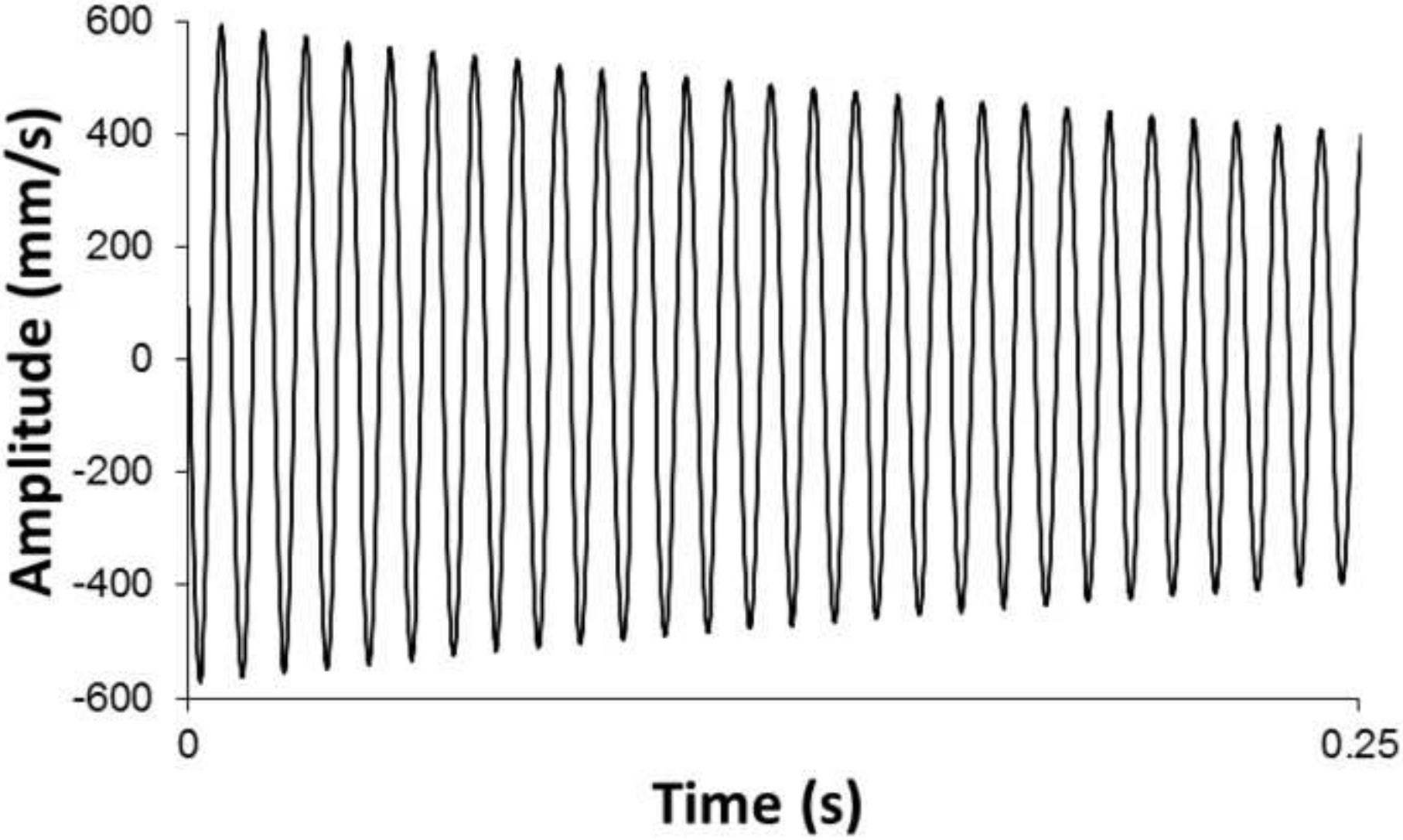

Figure 9 ALL_VERSIONS
Click here to download high resolution image

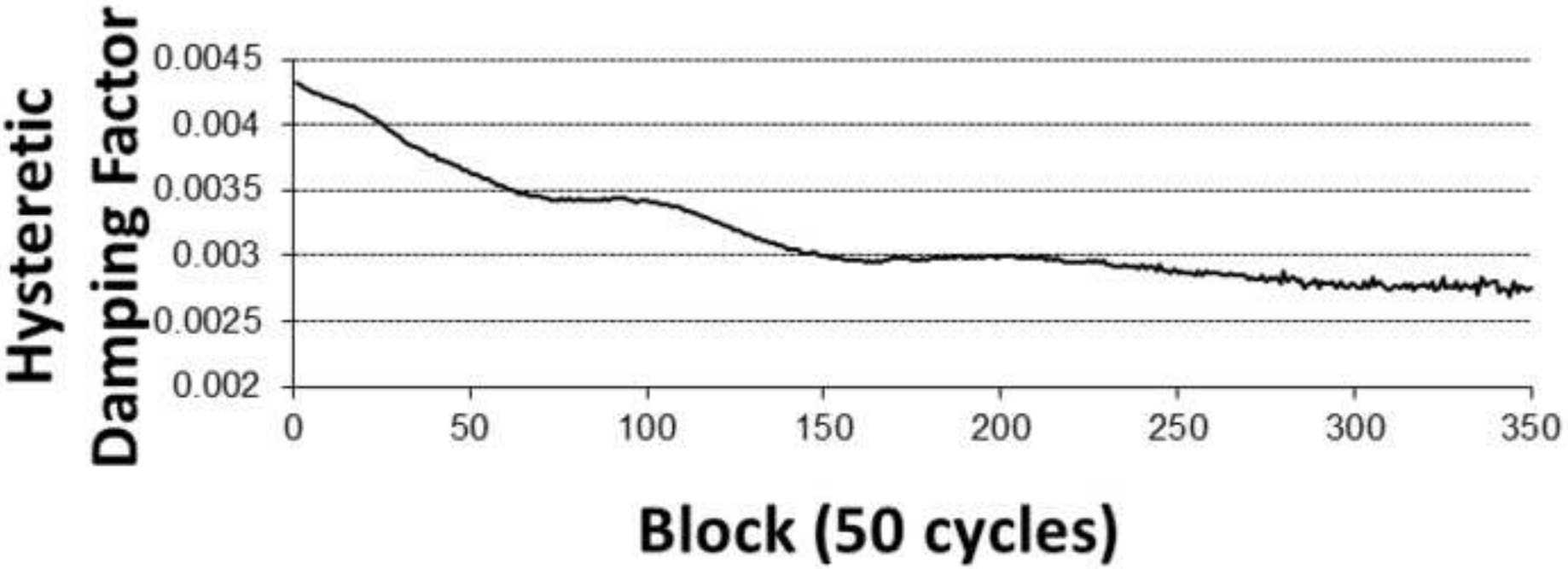

Figure 10 ALL_VERSIONS
Click here to download high resolution image